

DESIGN OF AN ULTRA-SENSITIVE MEMS FORCE SENSOR UTILIZING MODE LOCALIZATION IN WEAKLY COUPLED RESONATORS

C. Zhao¹, G. S. Wood¹, S. H. Pu^{1,2}, M. Kraft¹

¹ Nano Research Group, University of Southampton, School Electronics and Computer Science, Highfield Campus, Southampton, SO17 1BJ, United Kingdom

² University of Southampton Malaysia Campus, Nusajaya, 79000 Johor, Malaysia

Abstract — In this paper, the design of a novel ultrasensitive MEMS resonant force sensor utilizing a mode localization effect is presented. This new type of resonant sensor is constituted of several weakly coupled resonators and by measuring the amplitude ratio of designated resonators, a significant improvement in sensitivity is observed, compared to conventional frequency shift measurements. Furthermore, compared with conventional cantilever force sensors, the sensor is shown to be less constrained by the trade-off between sensitivity and stability along the axis of sensitivity, thus higher sensitivity and better stability can be achieved at the same time.

Keywords: Resonant sensor, Ultrasensitive force sensor, Mode localization, MEMS

I – Introduction

Over the last couple of decades, micro- and nano-fabricated devices have become widely used in force sensing applications, due to their high sensitivity, small form factor and low cost. Up to now, micro- and nano-scale cantilevers are the most attractive and widely used sensor types, one reason is their low springs stiffness enabling high sensitivity and good resolution [1, 2, 3, 4].

However, for non-contact force sensors (e.g. AFM), cantilevers with a low stiffness are not stable enough in the direction of measurement, causing unwanted “snapping down” when a large force gradient is present—an instability analogous to the “pull-in” of a MEMS parallel plate actuator, thus leading to inaccurate measurement [4]. Therefore resonant force sensing devices [3, 4] were developed. In principle, changes of exerted axial force alter the spring constant of the fixed-fixed beam, shifting the transverse vibration frequency. These resonant devices utilize this principle for force detection. With this method, the axial stiffness is significantly higher ($>500\text{N/m}$ [4] compared to a stiffness usually less than 1N/m of a typical cantilever [1, 2]). Thus the stability in the direction of force is increased. However, these sensors usually have lower sensitivity and resolution [3].

In general, there is a trade-off between sensitivity and stability in conventional force sensing techniques. Recently, a new sensing technique that makes use of a mode localization effect in weakly coupled resonators has shown good promise to overcome this trade-off.

Comparing with conventional resonators, these mode

localized two degree-of-freedom (DOF) sensors adopt a shift in eigenstates (resonance amplitudes) instead of frequency as the output signal. By sacrificing the quasi-digital output, this approach potentially can gain a substantial, that is two to three orders of magnitude, improvement in sensitivity [5, 6, 7]. By improving the sensitivity without sacrificing axial stiffness, such sensors are less constrained in terms of a trade-off between sensitivity and stability.

In this work, a three DOF system with further enhancement in sensitivity to the previously reported two DOF mode localized sensors is presented. The system adopts resonance amplitude ratio change as the output signal instead of normalized eigenstates shift. This potentially simplifies the required interface circuit.

II – Theory

A. Resonant Force Sensing

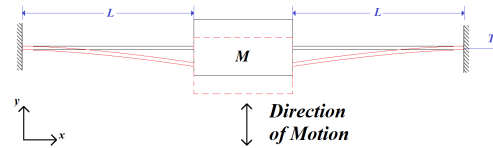


Figure 1: A resonator under axial tension.

For a resonator under axial tension, the mechanical characteristics of the beam can be derived [8]:

$$K_{eff} \approx \varphi \frac{EI}{L^3} + \sigma \frac{T}{L} \quad (1)$$

$$M_{eff} \approx \tau \rho A L + M \quad (2)$$

where E, ρ are the young's modulus and the density of the material, respectively, I is the second moment of inertia of the relevant cross section, L is the length of the beam, T is the axial tension force, A is the cross section area, and φ, σ and τ are three constants determined by the resonance mode and boundary conditions. For the beams shown in figure 1, the effective stiffness is:

$$K_{eff} \approx 12 \times \frac{EI}{L^3} + 1.2 \times \frac{T}{L} \quad (3)$$

It is clearly shown that when an axial force is exerted, only the stiffness changes. Therefore the resonator under axial tension force can be modeled as a axial-force-controlled spring with a constant mass, shown in fig-

$$\begin{bmatrix} M & 0 & 0 \\ 0 & M & 0 \\ 0 & 0 & M \end{bmatrix} \begin{bmatrix} \ddot{x}_1 \\ \ddot{x}_2 \\ \ddot{x}_3 \end{bmatrix} = \begin{bmatrix} -(K + \Delta K + K_c) & K_c & 0 \\ K_c & -(K_m + 2K_c) & K_c \\ 0 & K_c & -(K + K_c) \end{bmatrix} \begin{bmatrix} x_1 \\ x_2 \\ x_3 \end{bmatrix} \quad (4)$$

ure 2. This theory is combined with mode localization theory in our work.

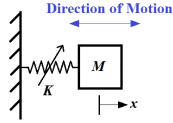


Figure 2: Tunable spring mass model of a resonator under axial tension. The tunable spring constant is controlled by the axial tension exerted.

B. Mode Localization in 3 DOF Force Sensor

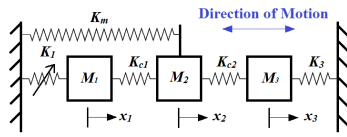


Figure 3: A spring-mass model of a 3 DOF force sensor. K_1 is the beam on which the force-to-be-measured is applied, thus it is tunable by the force.

Referring to figure 3 showing a coupled 3 DOF force sensor model, assume that $M_1 = M_2 = M_3 = M$, $K_{c1} = K_{c2} = K_c$, $K_2 = K$, $K_1 = K + \Delta K$ and $K_m \geq K$. The equations of motion are given in equation 4.

By solving equation 4, the amplitude ratio can be obtained. When $\Delta K = 0$, i.e. the unperturbed case, $x_3/x_1 = 1$ or -1 for the fundamental modes. When $\Delta K \neq 0$, i.e. a force is applied, the ratio is not 1 or -1 anymore, *mode localization* occurs in the sense that one of the resonators vibrates with a larger amplitude than the other. The change of ratio reflects the magnitude of the force. Assuming weak coupling, $K_c \ll K$, and small perturbations, $|\Delta K| \ll K$, in the mode of interest (i.e. in-phase mode), amplitude ratios of interest can be calculated as:

$$\frac{x_3}{x_1} \approx \frac{\gamma_1 \delta K + \sqrt{(\gamma_1 \delta K)^2 + 4}}{2}, \quad \Delta K \geq 0 \text{ and } |\Delta K| \ll K \quad (5)$$

$$\frac{x_1}{x_3} \approx \frac{-\gamma_1 \delta K + \sqrt{(\gamma_1 \delta K)^2 + 4}}{2}, \quad \Delta K < 0 \text{ and } |\Delta K| \ll K \quad (6)$$

where

$$\delta K = \frac{\Delta K}{K} \quad (7)$$

$$\gamma_1 = \frac{K(K_m - K + K_c)}{K_c^2} > 0 \quad (8)$$

Equation 5 is for positive and equation 6 is for negative perturbations.

C. Result Verification

MATLAB can be used to solve the eigenproblem in equation 4 without any assumptions, so by comparing the numerical results in equations 5 and 6 to the MATLAB direct solution, the error of the theory can be obtained. Figure 4 demonstrates the relative error.

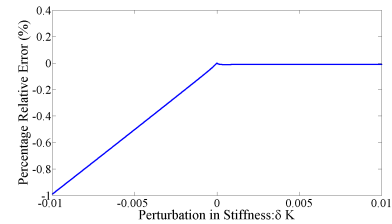


Figure 4: Relative error between analytical result and MATLAB calculation, calculation condition $M_1 = M_2 = M_3$, $K_m = 2K$, $K = 100K_c$.

Despite of the fact that when perturbation is negative, the estimations are less accurate than positive perturbations, it is observed that when the perturbation is very small (i.e. $|\Delta K| \ll K$), equations 5 and 6 can be regarded as accurate (with less than 1% relative error).

With the expressions verified, the following case of positive perturbations is mainly discussed, due to the symmetry of the two expressions.

D. Force Sensitivity of 3 DOF Force Sensor

The force sensitivity of the 3 DOF systems is:

$$S_{3DOF} = \frac{\partial \left(\frac{x_3}{x_1}, \frac{x_1}{x_3} \right)}{\partial (\delta K)} \frac{\partial (\delta K)}{\partial T} \quad (9)$$

It is therefore obtained from equations 3, 5 and 6:

$$0.6 \times \frac{\gamma_1}{KL} \leq S_{3DOF} \leq 1.2 \times \frac{\gamma_1}{KL} \quad (10)$$

By solving a similar eigenproblem of a 2 DOF system, the amplitude ratio can also be deduced, hence sensitivity can be obtained:

$$0.6 \times \frac{\gamma_2}{KL} \leq S_{2DOF} \leq 1.2 \times \frac{\gamma_2}{KL} \quad (11)$$

where

$$\gamma_2 = \frac{K}{K_c} \quad (12)$$

When K, K_c, L are identical, by comparing the maximum sensitivity that can be achieved in 2 DOF and 3 DOF systems, it is calculated that:

$$\frac{\max(S_{3DOF})}{\max(S_{2DOF})} = \frac{\gamma_1}{\gamma_2} = \frac{K_m - K + K_c}{K_c} \quad (13)$$

When K, K_c, L are identical, it is obvious that as long as it is designed that $K_c \ll K_m - K + K_c$, the sensitivity of a 3 DOF system shows a significant improvement from that of a 2 DOF system.

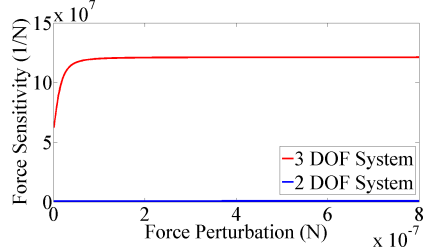


Figure 5: Force sensitivity plots of 3 DOF and 2 DOF systems. As an example, calculation in MATLAB is carried out with a condition of $M_1 = M_2 = M_3, K = 1 \text{ N/m}, K_m = 2 \text{ N/m}, K_c = 0.01 \text{ N/m}, L = 100 \mu\text{m}$. As expected, the 3 DOF system has 101 times higher sensitivity than 2 DOF system.

In addition to that, from equation 10, it is observed that the masses of the force sensor do not affect the sensitivity, therefore, lowering the resonance frequency by increasing mass will not lower its sensitivity.

III – Design and Simulation

A. Electrostatic Coupling

From previous theoretical derivations, it can be inferred that low coupling stiffness is desired. Hence a tunable electrostatic spring was chosen as a coupling mechanism. Over a small displacement, the effective spring constant can be expressed as [7]:

$$K_c \approx -\frac{V^2 \epsilon_0 \epsilon_r A_p}{d^3}, \quad \Delta x \ll d \quad (14)$$

where V is the voltage difference between two electrodes (i.e. the side areas of the proof masses), ϵ_0, ϵ_r are the dielectric constant of vacuum and relative dielectric constant, respectively, A_p is the effective cross sectional area of the electrodes and d is the gap between the electrodes.

B. Design of an Electrostatically Coupled 3 DOF Resonant Sensor

Each resonator in the design is comprised of a spring, which is a suspension beam, and a proof mass as shown in figure 6. Proof masses are used to obtain low resonant frequencies (in the kHz range), to simplify the interface circuitry while not losing sensitivity, and to make the proof masses less prone to random fabrication variations as one important assumption is that all masses are

equal. A larger proof mass also makes the mass of the beams negligible.

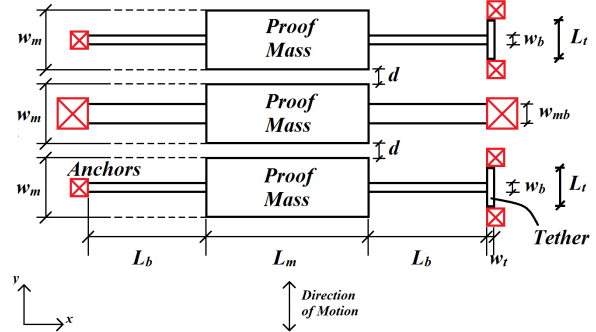


Figure 6: Design schematic (top view) of the 3 DOF force sensor, with geometrical parameters defined.

The 3 DOF design is composed of two identical resonators on either sides, and one more resonator in the middle, however with larger w_{mb} , so that when $K_c \ll K$, the stiffness of the center resonator satisfies $K_c \ll K_m - K$ as well. Tethers are added at the end of the resonators, so force can be applied.

The design has been built into 3D model. Figure 7 shows the 3D view of the design. The fabrication process will be a SOI process with a $50\mu\text{m}$ structural layer as described in [9]. In figure 7 the blue layer is the structural layer, while the red layer is the oxide and the grey layer is the handle wafer. The yellow surfaces in the inset and their counterparts are coupled through electrostatic force, therefore the gap between resonators can be seen as an electrostatic spring, with a spring constant shown in equation 14.

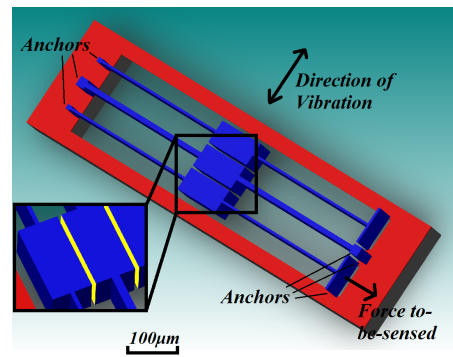


Figure 7: 3D view of the designed 3 DOF system. Inset shows the magnified view of the tagged area.

C. Simulation Results and Comparison with Theory

The design is simulated in Coventorware using finite element method (FEM). By applying a force on one of the resonators, perturbed resonance modes can be obtained, thus amplitude ratios are extracted from simulations. Figure 8 shows mode localization when

applying a tension force perturbation on the resonator on the left.

Table 1: Design parameters for the designed 3 DOF system.

| Parameters | Values | Remarks |
|------------|-----------------------|------------------------------------|
| L_b | 300 (μm) | All the beams have the same length |
| w_b | 5 (μm) | Width of beams on either side |
| w_{mb} | 10 (μm) | Width of beam in the middle |
| L_m | 100 (μm) | Three identical masses |
| w_m | 50 (μm) | |
| L_t | 50 (μm) | Tether length |
| w_t | 5 (μm) | Tether width |
| t | 50 (μm) | Device thickness |
| d | 5 (μm) | Coupling gap |
| f | $\sim 50\text{kHz}$ | Designed frequency |

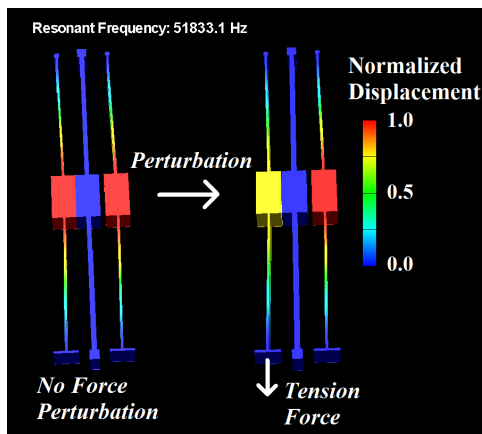


Figure 8: Localized mode in the 3 DOF system (right), with an exerted force of 50 nN compared to the unperturbed mode (left), while resonant frequency remains, at roughly 51.8 kHz.

The simulated result can be compared with theoretical analysis. This comparison is shown in figure 9.

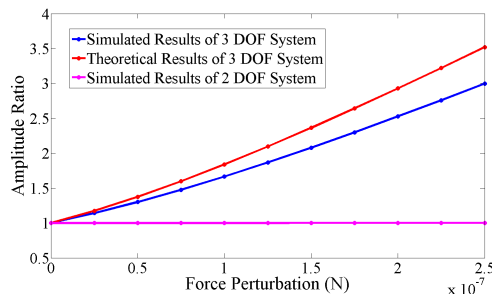


Figure 9: Simulated amplitude ratio with varying force perturbation and its comparison to theory and 2 DOF system simulation results. (Simulated $K/K_c = 65.38$.)

As can be seen, the simulation result agrees with the analytical modelling well (the maximum relative error in this simulation is approximately 16%). However, there is an increasing error occurring when the axial force increases. The main reason causing this

discrepancy is when the mode shape becomes localized to one of the resonators, the two coupling spring constants become unequal. The other reason causing the difference is that the three masses are not exactly identical as the middle resonator has wider suspension beams. For small perturbation (<25 nN), simulation and theory matches very well (within <5% error).

Furthermore, a 2 DOF system with identical design (K, M, K_c) is also simulated, and the results are also shown in figure 9. It is clear that the sensitivity of 3 DOF system is much higher than that of 2 DOF system as predicted. The sensitivity enhancement is calculated to be 3 orders of magnitude.

IV – Conclusion and Future Work

In this paper, a novel 3 DOF resonant force sensor utilizing mode localization is discussed in theory and simulated. An extension to the previous theories is provided and verified in this paper. According to the extended theory, compared with previous work with 2 DOF design, 3 DOF system is proved to be more sensitive, for the same stiffness and coupling spring constant. The design is simulated using finite element method, achieving good matching with theory. Moreover, it achieves another 3 orders of magnitude higher sensitivity than existing 2 DOF resonant force sensors. Future work will focus on the fabrication of an actual force sensor employing a 3 DOF resonator system.

References

- [1] G. Binning and C. F. Quate. *Physical Review Letters*, 56(9):930–933, 1986.
- [2] J. L. Arlett, J. R. Maloney, B. Gudlewski, M. Mulinex, and M. L. Roukes. *Nano Letters*, 6(5):1000–1006, 2006.
- [3] A. Stalder and U. Durig. *Review of Scientific Instruments*, 66(6):3576–3579, 1995.
- [4] J. A. Harley and T. W. Kenny. *Journal of Microelectromechanical Systems*, 10(3):434–441, 2001.
- [5] M. Spletzer, A. Raman, A. Q. Wu, X. Xu, and R. Reifenberger. *Applied Physics Letters*, 88(25):254102, 2006.
- [6] E. Gil-Santos, D. Ramos, A. Jana, M. Calleja, A. Raman, and J. Tamayo. *Nano letters*, 9(12):4122–4127, 2009.
- [7] P. Thiruvenkatanathan. PhD thesis, University of Cambridge, 2010.
- [8] S. S. Rao. *Mechanical Vibrations*. Pearson Education South Asia Pte Ltd., 5th edition, 2011.
- [9] I. Sari, I. Zeimpekis, and M Kraft. *Microelectronic Engineering*, 95:121–129, 2012.